DEUTSCHES ELEKTRONEN-SYNCHROTRON DESY

DESY 83-011
March 1983

RECENT RESULTS IN TWO PHOTON PHYSICS FROM JADE

by

T. Nozaki

Physikalisches Institut der Universität Heidelberg

ISSN 0418-9833

NOTKESTRASSE 85 · 2 HAMBURG 52

To be sure that your preprints are promptly included in the
HIGH ENERGY PHYSICS INDEX ,
send them to the following address (if possible by air mail) :

DESY
Bibliothek
Notkestrasse 85
2 Hamburg 52
Germany

DESY 83-011
March 1983

ISSN 0418-9833

Recent Results in Two Photon Physics from JADE(*)

by

T. Nozaki(**)

Physikalisches Institut der Universität Heidelberg

Heidelberg, Germany

Abstract

Two topics in two photon physics from JADE are reported: The measurement of the photon structure function F_2 and the analysis of single A_2 and f production in two photon reactions. The photon structure function F_2 was measured at an average Q^2 of 23 GeV^2 and compared with the predictions of leading and higher order QCD as well as of the quark parton model. The QCD scale parameter Λ was determined by these comparisons. The analysis of the processes $e^+e^- \to e^+e^-A_2$ ($A_2 \to \rho^\pm\pi^\mp$, $\rho^\pm \to \pi^\pm\pi^0$) and $e^+e^- \to e^+e^-f$ ($f \to \pi^0\pi^0$) is presented. Preliminary values of $\Gamma_{A_2\gamma\gamma}$ and $\Gamma_{f\gamma\gamma}$ are given.

(*) Talk given at the Gamma-Gamma Seminar at the University of Science and Technique of Languedoc, Montpellier, France, November, 1982.

(**) Now at University of Lancaster,Lancaster, England.

In this talk I will report on recent results in two photon physics obtained with the JADE detector at PETRA. The first topic is the analysis of the photon structure function F_2 at an average Q^2 of 23 Gev^2, which was recently published[1]. The second topic is the analysis of the production of single A_2 and f mesons in two photon reactions.

A measurement of the two photon initiated hadron production,

$$e^+e^- \to e^+ e^- + \text{hadrons} \qquad (1)$$

has been made under the single tag condition. The energy and the angle of one of the scattered electrons were measured by the two arrays of endcap lead glass counters[2], while the other electron was not detected. Under this single tag condition reaction (1) can be recognized as electron scattering off a quasi real photon radiated from the other initial electron (deep inelastic $e\gamma$ scattering).

In terms of the photon structure functions F_2 and F_L the cross section for deep inelastic electron photon scattering is given by [3]

$$d\sigma/dE'd(\cos\Theta) = (4\pi\alpha^2 E'/(Q^4 y)) \{ (1+(1-y)^2) F_2(x,Q^2) - (2 xy^2) F_L(y) \} \qquad (2)$$

Q^2 and the scaling variables x and y are given by: $Q^2 = 4 EE' \cdot \sin^2(\Theta/2)$, $x = Q^2/(Q^2 + W^2)$ and $y = 1-(E'/ E) \cdot \cos^2(\Theta/2)$, where E' and Θ are the energy and the polar angle of the tagged electron, respectively, and W is the total CM energy of the produced hadron system. Acordingly one can determine F_2 and F_L simultaneously from the measurement of reaction (1) if enough statistics are available. But with the present experimental conditions, namely low statistics (125 events) and small y^2 values ($\langle y^2 \rangle = 0.07$), only F_2 can be measured.

The hadronic two photon events of reaction (1) were selected by applying the following criteria:

a) The detection of an electron in one of the two arrays of endcap lead glass counters with an energy exceeding $0.5 \cdot E_{beam}$ in the angular range of Θ = 265-428 mrad. A track associated with the tagged lead glass cluster had to be seen in the central drift chamber.
b) The absence of a second high energy electron with an energy in excess of $0.25 \cdot E_{beam}$ elsewhere in the whole lead glass arrays.
c) The visible CM energy of the produced hadron system $W_{vis} > 1$ GeV (assuming all pions).
d) At least three additional charged tracks or two additional charged tracks plus at least one photon . A transverse (total) momentum > 0.1 GeV/c and $\cos\vartheta_t < 0.970$ were required for each charged track (photon),

respectively, where ϑ_i is the polar angle of the track(photon) with respect to the beam line.

e) A high energy photon which is emitted from an initial state electron and which converts before the central chamber, looks like a short track thus imitating a tagged electron. But the dE/dx of such a track is twice as large as that of a single electron. Acordingly the majority of the 1 γ annihilation background events were removed by making use of the dE/dx information from the central drift chamber[4], as well as the longitudinal momentum balance.

The data taken in the period from spring 1979 until summer 1981 have been analysed. The corresponding integrated luminosity is 20.2 pb^{-1} and beam energies are distributed between 13.8 and 18.4 GeV, with an average of 16.8 GeV.

176 events passed the above criteria and 125 events remained after subtraction of 51 background events. The data sample together with the details of the background events is compared with those of two other PETRA experiments in Table 1 [5,6]. The background is mainly due to the process $e^+e^- \to e^+e^-\tau^+\tau^-$. Q^2 and angular ranges for the three experiments are compared in Fig.1. Fig.2 shows a computer display of a $e^+e^- \to e^+e^-$+hadrons event.

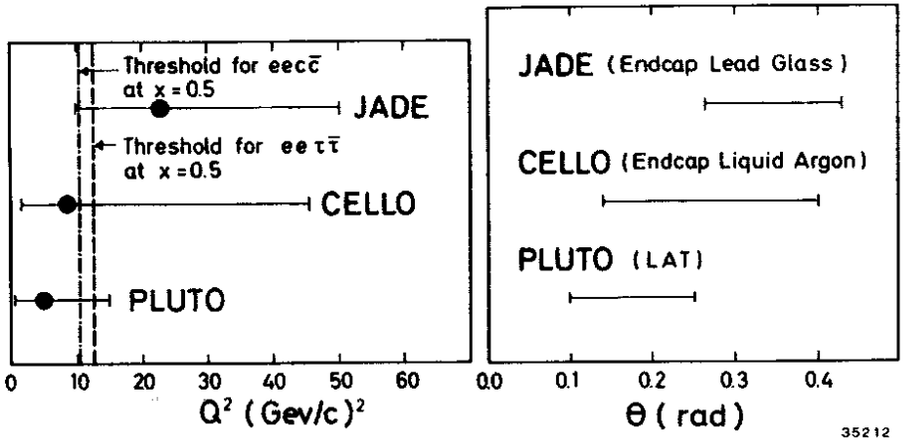

Fig.1 Q^2 and angular ranges of the tagged electron for three PETRA experiments.

	JADE	CELLO	PLUTO
• $< E_{beam} >$ (GeV)	16.8	17	15.5
• $\int$ L dt (pb^{-1})	20.2	11.2	2.5
• Observed events	176±13	305	117
• Background events	51±6	38	≤6.3
• $e^+e^- \to e^+e^-$h's events	125±15	267	111
• $< Q^2 >$ (GeV^2)	23	8.4	5

Background events

	JADE	CELLO	PLUTO
• $e^+e^- \to e^+e^-\tau^+\tau^-$	24.8±2.5	22	0
• $e^+e^- \to \tau^+\tau^-$	4.6±1.6	0	0
• Inelastic Compton	4.1±0.3	0	≤0.3
• Beam gas	3.8±1.1	0	5
• 1 γ annihilation	13.9±5.5	16	1

Table 1 Measurements of the two photon initiated hadron events are compared for three PETRA experiments.

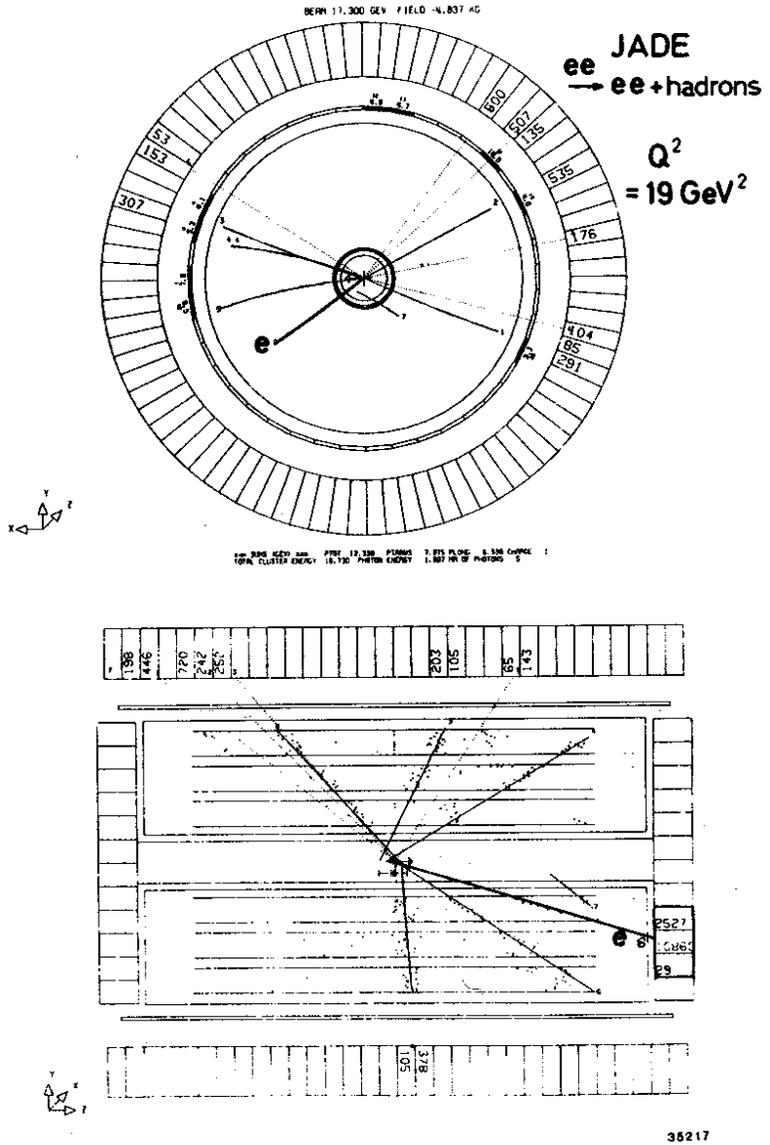

Fig.2 Computer display of a e^+e^- → e^+e^-+hadrons event in JADE. Solid lines are charged particles and dotted lines are photons. Energies deposited in the lead glass counters are indicated in MeV. The upper and lower figures show r-φ and side views, respectively.

F_2 is a function of x and Q^2 and we first study the x dependence of F_2 by plotting the x_{vis} distribution. x_{vis} is the measured x and is given by

$$x_{vis} = Q^2/(Q^2 + W^2_{vis}). \qquad (3)$$

Q^2 is calculated from the measured energy and polar angle of the scattered electron. W_{vis} is calculated by means of the measured momenta of charged tracks and photons assuming pion masses for all charged tracks. W_{vis} is on the average 30 % smaller than the true W due to the loss of particles outside the limited acceptance. In order to take into account this detection loss of particles as well as the resolution of the detector, a computer simulation program of reaction (1) was written. In this simulation first $e^+e^- \to e^+e^-q\bar{q}$ events were produced [7] according to various theoretical predictions of the F_2 function : Quark parton model (QPM) [8], leading order QCD (LOQCD)[9] and higher order QCD (HOQCD)[10]. These functions are shown in Fig.3 for $Q^2 = 23$ GeV^2.

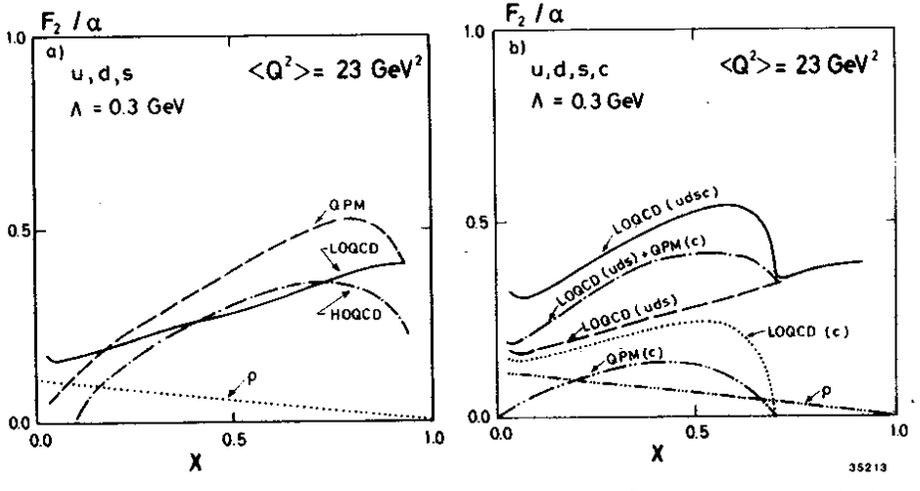

Fig.3 a) F_2/α as a function of x at Q^2=23 GeV^2. Solid curve = LOQCD (u,d,s) with Λ_{LO}=0.3 GeV. Dash-dotted curve = HOQCD (u,d,s) with $\Lambda_{\overline{MS}}$=0.3 GeV. Dashed curve = QPM (u,d,s). Dotted curve = ρ pole contribution[3].

b) F_2/α as a function of x at Q^2=23 GeV^2, including c quark contributions. Solid curve = LOQCD (u,d,s,c) with Λ_{LO}=0.3 GeV. Dash-dotted curve = LOQCD (u,d,s) with Λ_{LO} = 0.3 GeV plus QPM(c). Dashed curve = LOQCD (u,d,s) with Λ_{LO} = 0.3 GeV. Dotted curve = LOQCD (c) with Λ_{LO} = 0.3 GeV. Dash-doubly dotted curve = QPM (c). Dash-triply-dotted curve = ρ pole contribution.

The quark masses were assumed to be : $m_u = m_d = 300$ MeV/c^2 , $m_s = 500$ MeV/c^2 and $m_c = 1.6$ GeV/c^2. Then the quarks were fragmented via the standard Field Feynman fragmentation scheme [11] and momenta and angles of particles were smeared in accordance with the resolution of the detector.

The hadronic (vector meson like) component of F_2 can not be calculated by perturbative QCD and is usually estimated from a ρ dominance model[3] resulting in a const(1-x) function for F_2. At our high Q^2 values, this hadronic component is much smaller than the pointlike component especially at large x as seen in Fig.3b. In addition the angular distribution of hadrons from the ρ production is peaked more sharply in the beam direction than in $q\bar{q}$ production and thus the detection efficiency for the hadronic component is smaller than for the pointlike component. Accordingly, the hadronic component was neglected in the present Monte Carlo calculations.

For the higher order QCD (HOQCD), F_2 becomes negative ~const/x (const<0), in the small x region and in this region F_2 for HOQCD is not plotted in Fig.3. This negative value of F_2 might be compensated by the additional hadronic component of F_2[10,12]. Recently this cancellation was explicitely demonstrated with a new parametrization of the photon structure function based on a single additional nonperturbative parameter[13]. The contribution from this small x region was neglected in the Monte Carlo simulation for HOQCD.

The simulation of reaction (1) reproduced various observed distributions rather well. For instance, the resulting Q^2 distribution of the tagged electrons as well as the p_t^2 distributions of charged particles and photons for the leading order QCD (LOQCD) are compared with the data in Fig.4 and Fig.5, respectively. These LOQCD predictions for Λ = 0.3 GeV are in good agreement with the data.

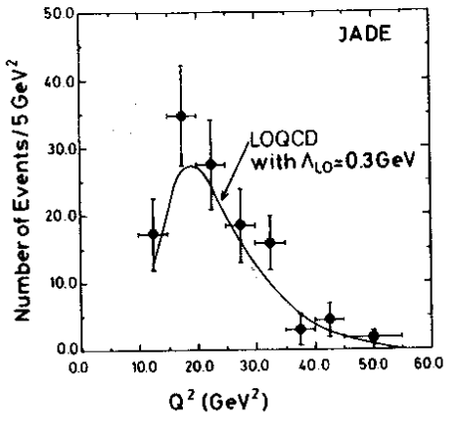

Fig.4 Q^2 distribution. Solid curve = LOQCD (u,d,s,c) with Λ_{LO}=0.3 GeV.

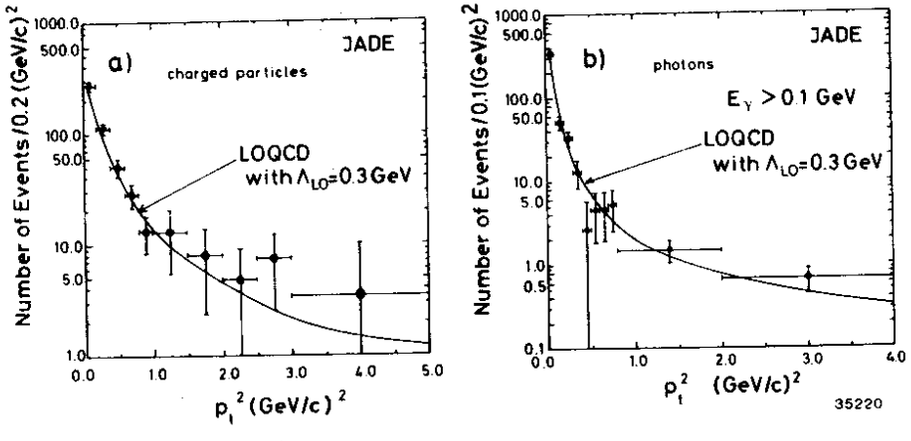

Fig.5 a) p_t^2 distribution of the produced charged particles. Solid curve = LOQCD (u,d,s,c) with Λ_{LO}=0.3 GeV.

b) p_t^2 distribution of the produced photons. Solid curve = LOQCD (u,d,s,c) with Λ_{LO}=0.3 GeV.

The x_{vis} distribution is shown in Fig.6a-6c. Fig.6a shows also the quark parton model prediction (QPM) together with the leading order (LOQCD) and higher order QCD (HOQCD) predictions, both for Λ = 0.3 GeV. All three curves provide a reasonable description of the data with the exception of the lowest x_{vis}-bin. The high data point in the lowest x_{vis}-bin might be due to the contribution from the hadronic component of the photon. The Monte Carlo curves of Fig.6 are quite sensitive to the parameter Λ as indicated in Fig.6b, since F_2 is proportional (approximately) to $\ln(Q^2/\Lambda^2)$ for LOQCD (HOQCD). This allows in principle the determination of Λ.

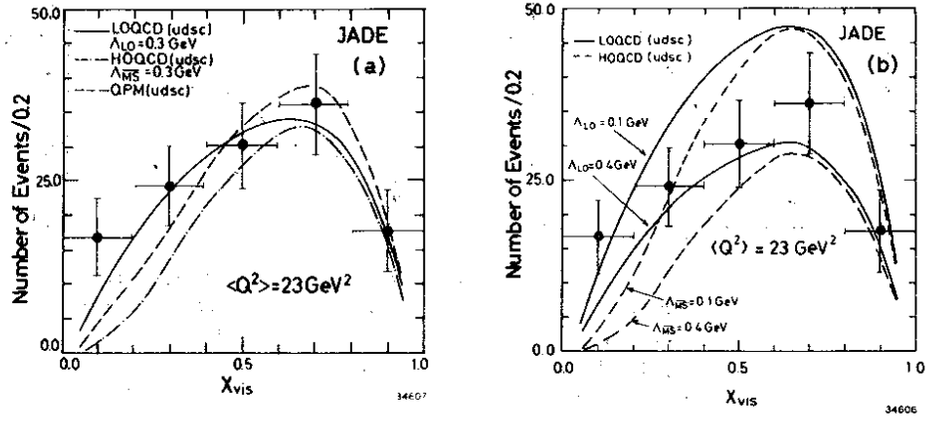

Fig.6 a) x_{vis} distribution. Solid curve = LOQCD (u,d,s,c) with Λ_{LO}=0.3 GeV. Dash-dotted curve = HOQCD (u,d,s,c) with $\Lambda_{\overline{MS}}$=0.3 GeV. Dashed curve = QPM (u,d,s,c).

b) x_{vis} distribution. Solid curves = LOQCD (u,d,s,c) with Λ_{LO} = 0.1 and 0.4 GeV. Dashed curves = HOQCD (u,d,s,c) with $\Lambda_{\overline{MS}}$ = 0.1 and 0.4 GeV.

Here two remarks must be made.

a) Only the high x_{vis} region (in the present analysis $x_{vis} > 0.4$) can be used for determination of Λ in order to reduce the hadronic component which contributes mainly in the small x region.

b) Although in our Q^2 range c quark production contributes nearly fully as seen in Fig.1, we do not have any adequate QCD calculations for c quark production. All the QCD calculations neglect the quark mass effects, an approximation not justified for the c quark.

One of these effects is the kinematical constraint of $W > 2\ m_q$, which limits the contribution from the c quark to F_2 above x= 0.7, at Q^2=23 GeV^2. Therefore the same F_2 function as for light quarks (u,d,s) was used for the c quark but the contribution from the x region corresponding to $W < 2\ m_c$ was neglected. This leads to the step structure around x=0.7 for the F_2 function as indicated in Fig.3b, where the distribution of Q^2 around 23 GeV^2 is taken into account. Also shown in Fig.3b is the F_2 function for which the light quark contribution was calculated by LOQCD but the c quark contribution was calculated by QPM, which includes quark mass effects. The corresponding predictions for the x_{vis} distribution are shown in Fig.6c. These curves give an estimate of the uncertainties introduced by the treatment of the c quark.

The step structure of the F_2 function in Fig.3b is not seen in Fig.6 due to the smearing effect in the conversion from x to x_{vis}, as indicated in Fig.7. Accordingly we can not make use of this step structure to identify the c quark contribution in the data.

If the c quark contribution is neglected completely then the QCD prediction decreases by about 40 % as seen in Fig.6c, resulting in a decrease of the estimated Λ value by a factor 3-4.

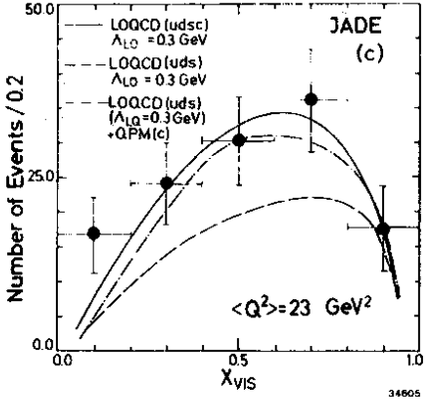

Fig.6 c) x_{vis} distribution. Solid curve = LOQCD (u,d,s,c) with Λ_{LO}=0.3 GeV. Dash-dotted curve = LOQCD (u,d,s) with Λ_{LO} = 0.3 GeV plus QPM(c). Dashed curve = LOQCD (u,d,s) with Λ_{LO} = 0.3 GeV.

The Λ values determined for various models are listed in Table 2. PLUTO [5] and CELLO [6] reported similar Λ values of 0.1-0.2 GeV and ~0.2 GeV, respectively, which were determined after subtracting the hadronic component from the data, since the latter contributes significantly in these two experiments

	Λ_{LO}	$\Lambda_{\overline{MS}}$
QCD (udsc)	$0.28^{+0.13}_{-0.09}$ GeV	$0.22^{+0.10}_{-0.07}$ GeV
QCD (uds)+QPM(c)	$0.21^{+0.17}_{-0.09}$ GeV	$0.18^{+0.12}_{-0.07}$ GeV
QCD (uds)	$0.07^{+0.05}_{-0.03}$ GeV	$0.06^{+0.05}_{-0.03}$ GeV

Table 2 Measured values of Λ_{LO}(LOQCD) and $\Lambda_{\overline{MS}}$(HOQCD) for three different models

Fig.7 shows the correlation between x_{vis} and x as calculated in the LOQCD Monte Carlo simulation. As seen in Fig.7, x_{vis} is larger than the true x due to the detection loss of particles and the average difference between x_{vis} and x is a function of x, but the difference fluctuates significantly event by event. Therefore in order to deduce the true x distribution from the x_{vis} distribution more statistics is needed.

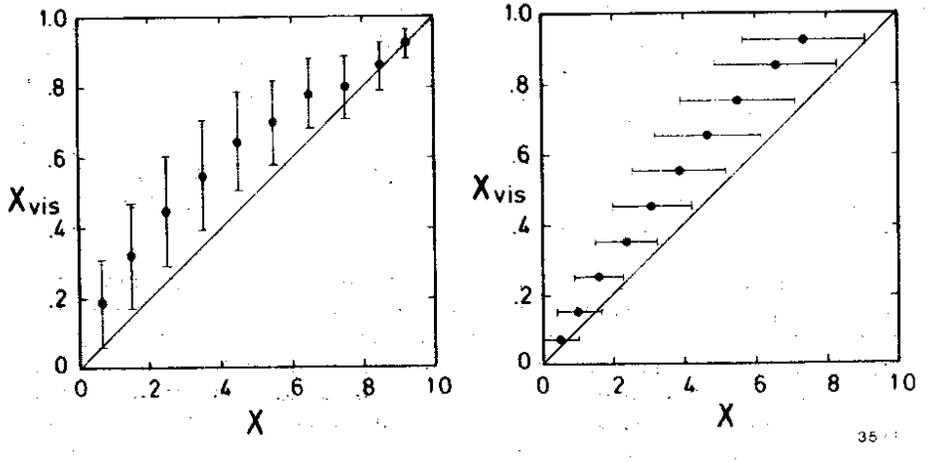

Fig.7 Correlation between x and x_{vis} calculated in LOQCD. Error bars correspond to one standard deviation

The Q^2 dependence of F_2 is now discussed. The pointlike component of F_2 is predicted to have a $\ln(Q^2)$ dependence for fixed x. A definite prediction of the Q^2 dependence of the hadronic component is not given by present theories and usually no dependence is assumed[3].

Fig.8 shows the Q^2 dependence of the function F_2 averaged over the range $x_{vis} > 0.3$. This x_{vis} cut was introduced to reduce the contribution coming from the hadronic component as well as to reduce the correlation between x and Q^2. Also shown in Fig.8 are the results of similar analyses at smaller Q^2 by PLUTO [5] and CELLO [6]. Data are compared with the LOQCD prediction with and without c quark contribution for Λ=0.3 GeV. The JADE data are consistent with these predictions, while the lower Q^2 points are located above these curves. This might be due to the hadronic contribution to F_2 which is expected to be more significant at smaller Q^2.

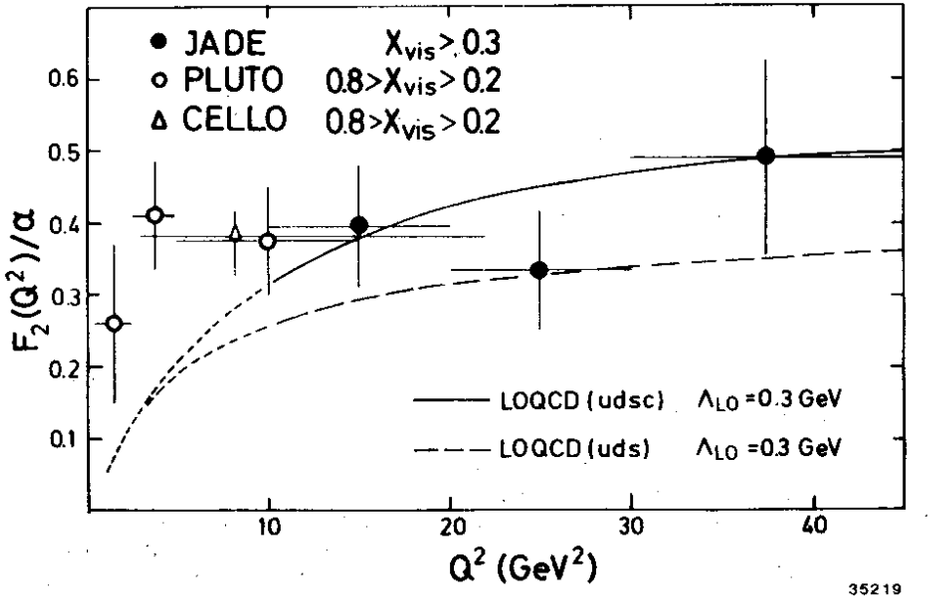

Fig.8 F_2/α as a function of Q^2. Full circles(JADE data)=$F_2(x,Q^2)/\alpha$ averaged over x_{vis}> 0.3. Open circles(PLUTO data)=$F_2(x,Q^2)/\alpha$ averaged over 0.2< x_{vis}< 0.8. Open triangle(CELLO data)=$F_2(x,Q^2)/\alpha$ averaged over 0.2< x_{vis}<0.8. Solid curve = LOQCD (u,d,s,c) with Λ_{LO}=0.3 GeV. Dashed curve = LOQCD (u,d,s) with Λ_{LO}=0.3 GeV.

We now come to the second topic, the production of single A_2 and f mesons in two photon reactions. The diagram of these processes is shown in Fig.9

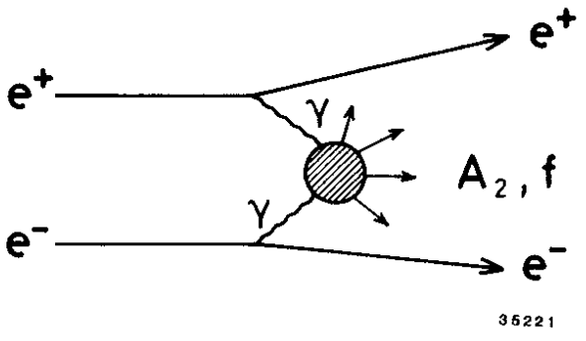

Fig.9 Diagram for the reactions $e^+e^- \to e^+e^- A_2$ and $e^+e^- \to e^+e^- f$.

Studying the $\pi^+\pi^-\gamma\gamma$ final state from the decay chain of $A_2 \to \rho^\pm\pi^\mp \to \pi^+\pi^-\pi^0$, a preliminary value of 0.63±0.08(stat.)±0.11(syst.) keV for the radiative width of A_2, $\Gamma_{A_2\gamma\gamma}$, was obtained earlier [14] with an integrated luminosity of 36 pb^{-1}. Since then we have accumulated about twice the luminosity and an extended analysis is in progress The value of the radiative width of A_2 depends significantly on the decay angular distribution of A_2 which is determined by the helicity state of A_2. The above value of the radiative width was determined under the assumption of A_2 being produced with pure helicity 2 in accordance with the theoretical expectations[15]. The analysis is not yet finished and here we show only the mass spectra of $\gamma\gamma$, $\pi^\pm\pi^0$ and of $\pi^+\pi^-\pi^0$ for an integrated luminosity of 68 pb^{-1} in Fig.9. In Fig.9b and c only events from the π^0 mass band indicated in Fig.9a are included. The two photons are constrained to the π^0 mass and a cut $p_t^2 < 0.36$ (GeV/c)^2 has been applied for the 3π system. Prominent $\rho^\pm$ and A_2 peaks are seen. The shaded histogram in Fig.9c includes all events with at least one $\pi^\pm\pi^0$ combination within the $\rho^\pm$ band indicated in Fig.9b.

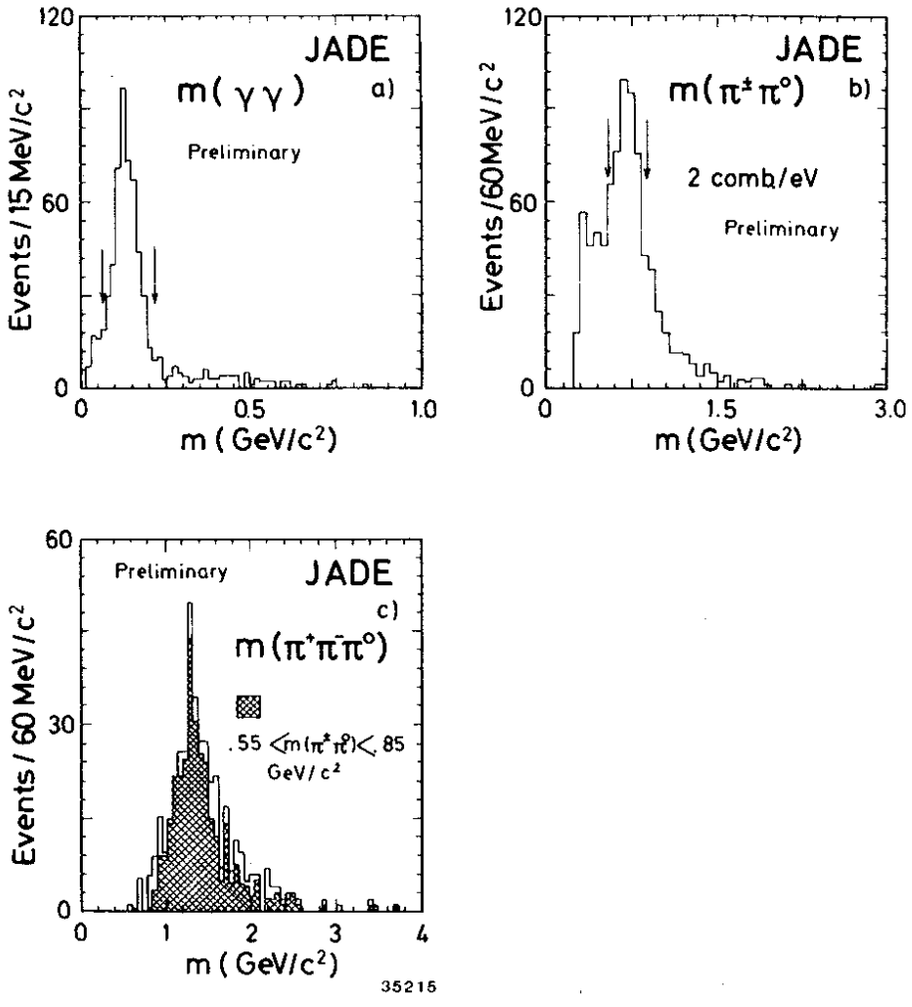

Fig.10 Invariant mass spectra for the reaction $e^+e^- \to e^+e^-\pi^+\pi^-\gamma\gamma$.
a) m($\gamma\gamma$). Arrows show the π^0 mass band.
b) m($\pi^\pm\pi^0$). Arrows show the $\rho^\pm$ mass band.
c) m($\pi^+\pi^-\pi^0$)

The resonance production of f has usually been studied by looking at the charged decay mode, $f \to \pi^+\pi^-$[16,17,18]. There are, however, some difficulties in these analyses. In addition to the large QED background, a large continuum was observed in the $\pi^+\pi^-$ mass spectrum and it was found to rise rapidly under and below the f mass. Furthermore the f mass was found to be smaller than the table value, 1273 MeV[19], when a simple Born term calculation was used for the estimation of the continuum. Although this mass shift of about 50 MeV seems to be understood in a recent sophisticated analysis based on the unitarized Born ansatz[18,20], a simpler and theory independent determination of the radiative width of f can be obtained by looking at the neutral decay mode, $f \to \pi^0\pi^0$. No large background is expected in this channel. The first measurement of this decay mode was done with the Crystal Ball[21]. The JADE Collaboration has installed a new neutral trigger scheme since the beginning of 1982 and measured the process $e^+e^- \to e^+e^-\pi^0\pi^0$. The events were simply selected by demanding four photons with energies > 100 MeV in the angular range of $|\cos\vartheta| < 0.76$. One example of $f \to \pi^0\pi^0$ is shown in Fig.11.

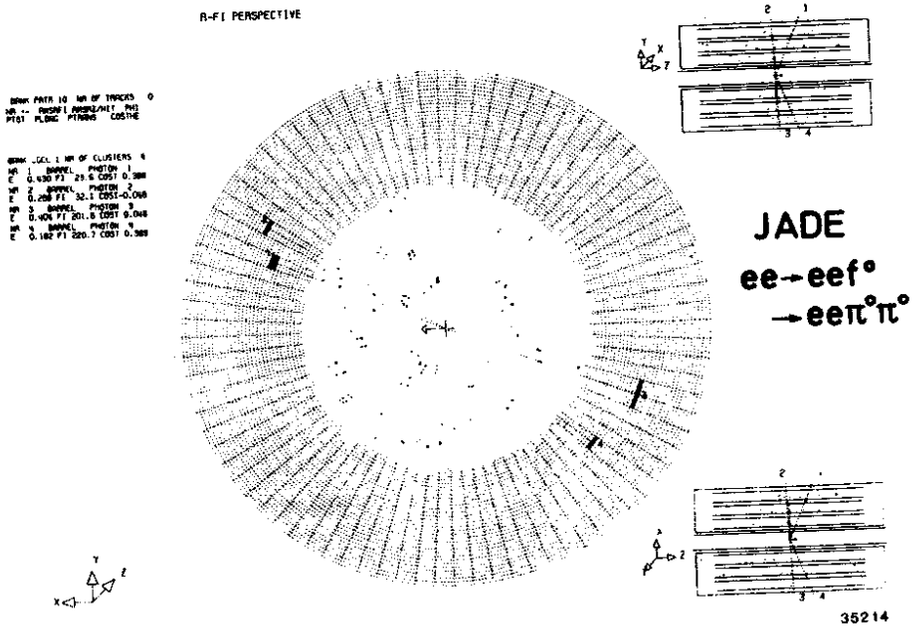

Fig.11 Computer display of a $f \to \pi^0\pi^0$ event. Dotted lines indicate photons. Also shown is the inside surface of the central lead glass cylinder

Fig.12a-b show the mass spectra of $\gamma\gamma$ and of $\pi^0\pi^0$ for an integrated luminosity of 33 pb^{-1}. In Fig.12b only events with two opposite $\gamma\gamma$ combinations, each of which lies in the π^0 band indicated in Fig.12a, are included. The two photon combinations are constrained to the π^0 mass and a cut $p_t^2 < 0.12$ (GeV/c)^2 has been applied to the resulting $\pi^0\pi^0$ system. A mass and width determination together with a helicity analysis are under study, but the data seem to be consistent with table values. Using data corresponding to an integrated luminosity of 24 pb^{-1}, a preliminary value of the radiative width of f was reported, $\Gamma_{f\gamma\gamma}$= 2.3 ± 0.2(stat.) ± 0.5(syst.) keV, under the assumption of a helicity 2 state for f[22].

SU(3) with ideal mixing predicts R= $\Gamma_{A_2\gamma\gamma}/\Gamma_{f\gamma\gamma}$=0.36, mass differences not considered. Our results give R=0.27±0.04(stat.)±0.08(syst.), which is consistent with this prediction.
The $\Gamma_{A_2\gamma\gamma}$ value agrees well with the other experimental results[21,23]. Also the $\Gamma_{f\gamma\gamma}$ value agrees well with the Crystal Ball result, $\Gamma_{f\gamma\gamma}$ =2.7+0.6-0.4(stat.)±0.6(syst.) keV [21], as well as with various measurements using the charged decay mode[16,17,18].

Summary

The photon structure function F_2 was measured at an average Q^2 of 23 GeV^2 and was found to be well described by leading order QCD without the vector meson like contribution in the whole x_{vis} region. Also the quark parton model as well as higher order QCD predictions without the vector meson like contribution agree well with the data except in the small x_{vis} region. The QCD parameter Λ was determined to be $\Lambda_{\overline{MS}}$ = 0.18 (+0.12,-0.07) GeV for higher order QCD. The Q^2 dependence of F_2 was found to be consistent with the ln(Q^2) dependence predicted by leading order QCD.
An analysis is in progress for the $e^+e^- \to e^+e^-A_2$ ($A_2 \to \rho^\pm\pi^\mp$, $\rho^\pm \to \pi^\pm\pi^0$) and $e^+e^- \to e^+e^-f$ ($f \to \pi^0\pi^0$) processes. Preliminary values for the radiative widths are $\Gamma_{A_2\gamma\gamma}$= 0.63±0.08(stat.)±0.11(syst.) keV and $\Gamma_{f\gamma\gamma}$= 2.3±0.2(stat.)±0.5(syst.) keV.

Acknowledgements

I wish to thank J. Olsson and T.F.Walsh for many useful discussions. I also thank G.Mennessier and the Organising Committee at Montpellier for an enjoyable time at Montpellier.

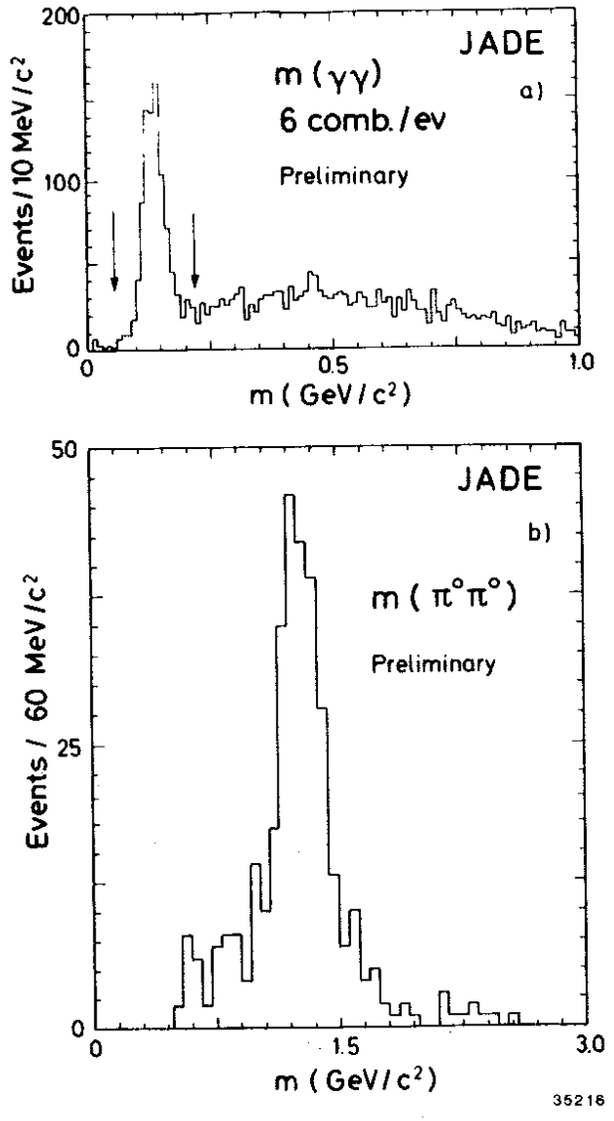

Fig.12 Invariant mass spectra for the reaction $e^+e^- \to e^+e^-\gamma\gamma\gamma\gamma$.
a) m($\gamma\gamma$). Arrows show the π^0 mass band.
b) m($\pi^0\pi^0$).

References

1. JADE Collaboration, W.Bartel et al., Phys.Lett 121B(1983)203.

2. JADE Collaboration, W.Bartel et al., Phys.Lett. 88B(1979)171.
ibid., 92B(1980)206 and 99B(1981)277.

3. C.Petersen,T.F.Walsh and P.M.Zerwas, Nucl.Phys. B174(1980)424.

4. H.Drumm et al., Nucl. Inst. and Meth., 176(1980)333.
J.Heintze, Nucl. Inst. and Meth., 196(1982)293.
A.Wagner, Proc. of the Int. Conf. on Instrumentation for Colliding Beam Physics, SLAC 1982, SLAC-Report 250,p76.

5. PLUTO Collaboration, Ch.Berger et al., Phys.Lett. 107B(1981)168.

6. CELLO Collaboration, Contribution to XXIst Inter. Conf. on High Energy Physics 1982 (Paris).

7. S.Kawabata, Program Write-Up(1982), unpublished.

8. C.T.Hill and G.G.Ross, Nucl.Phys. B148(1979)373.

9. E.Witten, Nucl.Phys. B120(1977)189.

10. T.Uematsu and T.F.Walsh, Nucl.Phys. B199(1982)93.

11. R.D.Field and R P.Feynman, Nucl.Phys. B136(1978)1.

12. W.A.Bardeen, Proc. of the 1981 Int. Symp. on Lepton and Photon Interactions at High Energies, Bonn 1981,p432.

13. I.Antoniadis and G.Grunberg, These proceedings.

14. J.E.Olsson, Proc. of the XVIIth Rencontre de Moriond, Les Arcs,Savoie,France, March 1982.

15. J.Babcock and J.L.Rosner, Phys.Rev. D14(1976)1286.
P.Grassberger and R.Kögerler, Nuc.Phys. B106(1976)451.
J.L.Rosner, Phys.Rev. 11(1974)189.
B.Schrempp-Otto et al., Phys.Lett. 36B(1971)463.
M.Greco, Lecture Notes in Physics(1980)311.

16. PLUTO Collaboration, Ch.Berger et al., Phys.Lett. 94B(1979)254.
TASSO Collaboration, R.Brandelik et al., Z.f.Physik C10(1981)117.
MARK II Collaboration, A.Roussarie et al., Phys.Lett.105B(1981)304

17. D.Cords, Talk given at the 1982 SLAC Summer Institute on Particle Physics, DESY 82-083, and to be published in the proceedings.

18. CELLO collaboration, Results presented by J.Field at this Seminar.

19. Particle Data Group, Phys.Lett. 111B(1982)1.

20. G.Mennessier, Z.f.Physik.C16(1982)241.

21. C. Edwards et al., Phys.Lett. 110B(1982) 82.

22. JADE Collaboration, Contribution to XXIst Inter. Conf. on High Energy Physics 1982 (Paris).

23. CELLO Collaboration, H.J.Behrend et al., Phys.Lett.114B(1982)378.